OPEN

Oncogene (2016) **35,** 1965–1976

www.nature.com/onc

ORIGINAL ARTICLE

The oncofusion protein FUS–ERG targets key hematopoietic regulators and modulates the all-*trans* retinoic acid signaling pathway in t(16;21) acute myeloid leukemia

AM Sotoca, KHM Prange, B Reijnders, A Mandoli, LN Nguyen, HG Stunnenberg and JHA Martens

The ETS transcription factor ERG has been implicated as a major regulator of both normal and aberrant hematopoiesis. In acute myeloid leukemias harboring t(16;21), ERG function is deregulated due to a fusion with FUS/TLS resulting in the expression of a FUS–ERG oncofusion protein. How this oncofusion protein deregulates the normal ERG transcription program is unclear. Here, we show that FUS–ERG acts in the context of a heptad of proteins (ERG, FLI1, GATA2, LYL1, LMO2, RUNX1 and TAL1) central to proper expression of genes involved in maintaining a stem cell hematopoietic phenotype. Moreover, in t(16;21) FUS–ERG co-occupies genomic regions bound by the nuclear receptor heterodimer RXR:RARA inhibiting target gene expression and interfering with hematopoietic differentiation. All-*trans* retinoic acid treatment of t(16;21) cells as well as FUS–ERG knockdown alleviate the myeloid-differentiation block. Together, the results suggest that FUS–ERG acts as a transcriptional repressor of the retinoic acid signaling pathway.

Oncogene (2016) **35,** 1965–1976; doi:10.1038/onc.2015.261; published online 6 July 2015

INTRODUCTION

Members of the large E-twenty-six-specific (ETS) protein family are winged helix–turn–helix DNA-binding domain transcription factors that have diverse functions and activities in physiology and oncogenesis, among which normal and aberrant hematopoiesis.[1] ERG (V-ets avian erythroblastosis virus E26 oncogene homolog), a hallmark ETS factor protein, is known to have a critical role in establishing definitive hematopoiesis and is required for normal megakaryopoiesis. Truncated forms of ERG due to oncogenic fusion translocations have been associated with multiple cancers such as Ewing's sarcoma (EWS–ERG), prostate cancer (TMPRSS2–ERG) and acute myeloid leukemia (FUS–ERG; ELF3–ERG).[2–4]

The *FUS–ERG* chimeric oncogene has been associated with acute myeloid leukemias (AMLs) carrying the non-random t(16;21)(p11;q22) chromosomal aberration. The resulting fusion protein retains the N-terminal domain of FUS/TLS (fused in sarcoma/translocated in liposarcoma) protein, and the C-terminal domain is replaced by the ETS motif-DNA-binding domain of ERG.[5] *In vitro* experiments suggest that the FUS/TLS fusion domain (TFD) regulates the DNA-binding activity of the FUS–ERG chimeric protein, which as a result shows weaker transcriptional activation properties compared with normal ERG proteins.[6] However, whether this mechanism also works *in vivo* is still unclear.

The normal *FUS* gene encodes an RNA-binding protein that serves in transcription regulation and RNA metabolism.[7] Both the amino- and the carboxy-terminal regions of FUS/TLS containing the conserved RNA-binding motifs are needed for poly(G)-specific RNA-binding activity. In addition, analysis of TLS–ERG mutants showed that the first 173 amino acids of the FUS/TLS N terminus comprise a subdomain that mediates interaction with RNAPII,[8,9] suggesting a direct role in transcriptional regulation and/or transcription-coupled RNA processing. A role in transcription regulation was further suggested by the finding that the N-terminal part of FUS binds retinoid-x receptor (RXR).[10–12] Finally, it has been shown that the C terminus of FUS inhibits DNA binding and transcription activation of SPI1 (PU.1).[13,14]

FUS expression is downregulated in the early stages of ATRA-induced granulocytic differentiation of HL60 leukemic cells.[15,16] Furthermore, a knockout study showed that *Fus* null mice have an increased number of granulocytes.[17] Another study with *Fus*-deficient mice showed that $Fus^{-/-}$ fetal livers developed normally, except for a mild reduction in numbers of hematopoietic stem and progenitor cells compared with wild type (WT).[18] These findings suggest a role for FUS in regulating hematopoietic stem cell self-renewal and terminal differentiation along the myeloid lineage.[19]

ERG has also been associated with aberrant hematopoiesis. High expression of ERG is linked with poor prognosis in a subgroup of leukemia patients with AML and acute T-lymphoblastic leukemia.[2,20,21] In addition, correct *Erg* gene dosage is critical for the maintenance of hematopoietic stem cell function. Mice homozygous for the loss-of-function Erg^{Mld2} mutation die at midgestation, with a profound defect in definitive hematopoiesis suggesting an essential role in hematopoietic stem cell self-renewal.[22–25]

Still, how FUS–ERG fusion protein may lead to cellular abnormalities by deregulating normal ERG gene transcription *in vivo* is not understood. Therefore, in the present study we used massive parallel sequencing of chromatin immunoprecipitates (chromatin immunoprecipitation-sequencing (ChIP-seq)) and quantitative sequencing of transcripts (RNA-seq) for identification of FUS–ERG-binding sites in t(16;21) AML cells. We found that FUS–ERG mainly binds non-promoter regions in a complex

Department of Molecular Biology, Faculty of Science, Nijmegen Centre for Molecular Life Sciences, Radboud University, Nijmegen, The Netherlands. Correspondence: Dr J Martens, Department of Molecular Biology, Faculty of Science, Nijmegen Centre for Molecular Life Sciences, Radboud University, FNWI, Geert Grooteplein 28, 6500 HB Nijmegen, Gelderland, Netherlands.
E-mail: j.martens@ncmls.ru.nl
Received 3 December 2014; revised 28 April 2015; accepted 5 June 2015; published online 6 July 2015

consisting of other ETS factors, GATA2, LMO2, LYL1, RUNX1, TAL1 and RNAPII. Interestingly, we noticed that apart from interacting with RXR, FUS–ERG also colocalizes to similar regions as the nuclear receptor RARA. Treatment with ATRA resulted in reduced FUS–ERG binding and higher expression of target genes, suggesting that the role of FUS–ERG in leukemogenesis relates to repressing the ATRA signaling pathway.

RESULTS

FUS–ERG expression in leukemic cells

The reciprocal translocation t(16;21)(p11;q22) is a rare abnormality associated with AML and present in the TSU-1621-MT and YHN-1 cells, a M4 and M1 AML type, respectively, according to the French-American-British classification. To validate gene expression arising from the translocation, we examined expression of FUS–ERG messenger RNA (mRNA) by reverse transcriptase–PCR (RT–PCR). Using primers that recognize exon 6 from FUS and exon 10 from *ERG*[26] (Figure 1a), we were able to confirm the expression of the oncofusion gene in the TSU-1621-MT and YNH-1 cells (Figure 1b), whereas it is not expressed in KG-1 and U937 cells that do not harbor this translocation.

To assess whether the fusion of *ERG* to *FUS* would affect WT *ERG* or *FUS*, we extended the quantitative PCR (qPCR) and analyzed the relative expression levels of the fusion gene as compared with the WT. This analysis revealed that WT *FUS* (FUS4-5) levels are comparable in all four cell types, whereas *ERG* levels are comparable in TSU, YNH-1 and KG-1 cells, but not detectable in U937. Western blot analysis using a C-terminal ERG antibody and a N-terminal FUS antibody confirmed the presence of high levels of FUS, and expression of FUS–ERG and ERG proteins in the nucleus of TSU-1621-MT cells (Figure 1c), whereas both FUS–ERG as well as WT ERG are not present in the U937 cells, corroborating the RT–qPCR results.

ERG-fusion-specific binding in cancer

The t(16;21) fusion results in aberrant expression of ERG in AML. ERG is also involved in translocations underlying prostate cancer (TMPRSS2–ERG) and Ewing's sarcoma (EWS–ERG).[27] To examine whether a common ERG cancer signature could be observed, we used an ERG antibody (recognizing the C-terminal region) in ChIP-seq experiments in the TSU-1621-MT leukemic cells and compared the profile with the ERG-binding profiles resulting from expression of TMPRSS–ERG in VCaP (prostate cancer) and EWS–ERG in CADO-ES1 cells[28,29] (Figure 1d). We used MACS2[30] at a *P*-value cutoff of 10^{-6} to identify all ERG-binding regions in TSU-1621-MT and EWS–ERG in CADO-ES1 (Ewing's sarcoma) cells and identified 31 596, 32 406 and 17 469 ERG-binding regions from TSU-1621-MT, VCaP and CADO-ES1 cells, respectively. Between TSU-1621-MT and VCaP cells, we identified a 35% overlap (11 116 binding sites), whereas only an overlap of 1% (404 binding sites) was found between EWS–ERG- and FUS–ERG-expressing cells. Intersection of the three data sets revealed an overlap of 148 peaks, representing mainly promoter regions associated with genes belonging to the Jak-STAT signaling and Wnt signaling pathways (*P*-values $5E^{-04}$ and $6E^{-04}$, respectively; data not shown).

The low overlap between the different ERG profiles suggests that ERG binds to different genomic loci depending on the cell type. To examine whether the aberrant ERG expression in t(16;21) AML would reflect ERG binding in other AML subtypes, we compared ERG binding in TSU-1621-MT cells with those in SKNO-1 and ME-1 cells, two cell lines representative of the t(8;21) and inv (16) translocation, respectively. Overlapping the binding regions of the three leukemic cell lines revealed a large common set of 17 750 regions (Figure 1e). As these AML common regions potentially represent key binding sites for ERG-induced leukemic transformation, we performed functional analysis of the associated genes. This revealed high enrichment scores (>10) for genes involved in regulation of the cell cycle (Figure 1f), suggesting the involvement of ERG target genes in deregulation of normal cell proliferation.

FUS–ERG targets ETS factor sites in promoter and enhancer regions

To identify potential FUS–ERG-binding sites, we extended our ChIP-seq analyses and included an antibody recognizing the N terminus of the FUS protein. Using the same peak-calling settings as above allowed the identification of 16 533 FUS-occupied regions in TSU-1621-MT cells. A total of 10 364 binding regions were found that overlapped between FUS and ERG, for example, at ITGAM and CSF3R promoter and enhancer regions, potentially representing FUS–ERG-binding sites (Figures 2a and b). A subset of these binding sites was validated through re-ChIP experiments on targeted loci, confirming that the two parts of the fusion protein occupy the same genomic region (Supplementary Figure 1). Moreover, transfecting a flag-tagged FUS–ERG followed by ChIP–qPCR in U937 cells, which do not express the fusion, showed binding at target sites identified in TSU-1621-MT cells (Supplementary Figure 2), confirming that the fusion protein can bind to these DNA regions.

To investigate whether WT FUS might colocalize with ERG, we extended our ChIP-seq analysis and examined binding of FUS at ERG-occupied regions in the SKNO-1 and ME-1 cells (Supplementary Figure 3). This analysis revealed enrichments of the FUS signal at ERG-binding sites in these two AML cell types, suggesting that WT FUS might also colocalize with ERG in other AMLs. Together these results suggest that in TSU-1621-MT cells due to the fusion of FUS and ERG, the interaction of these two proteins is stabilized.

The putative FUS–ERG-occupied regions in TSU-1621-MT cells are predominantly located in non-promoter, mostly intergenic regions (Figure 2c), whereas ERG peaks not overlapping with FUS (and likely representing WT ERG binding) show a higher percentage localized to promoter regions. Motif analysis of the FUS–ERG-binding sites revealed that the ETS factor core motif GGAAG was enriched in nearly all of the binding sites (Figure 2d). In addition to the ETS motif, the RUNX1 motif was also found to be enriched in FUS–ERG-binding sites, suggesting FUS–ERG is involved in aberrant regulation of RUNX1 target genes. Motif analysis of the 6169 FUS-only peaks surprisingly also revealed enrichment/presence of the ETS transcription factor motif. It was previously suggested that WT FUS binding to DNA could be mediated by interaction with SPI1.[13,14] Indeed, including a SPI1 ChIP-seq in our analysis revealed SPI1 enrichment at all FUS-only-binding sites (Supplementary Figure 4), suggesting that non-fused FUS recruitment to DNA might in part be ETS factor dependent.

FUS has been suggested to multimerize through its N-terminal domain,[31] suggesting that this property might also be present in the FUS–ERG fusion protein. Such oligomerization could be strengthened by the presence of multiple binding motifs for ERG. To inspect whether multiple ETS motifs are present in FUS–ERG-binding sites, we examined the number of motifs present within one peak (Figure 2e). In addition, we examined the number of RUNX1 motifs. This revealed that within one FUS–ERG-occupied region, generally one RUNX1 but multiple ETS motifs can be detected, suggesting that FUS–ERG may act in an oligomeric complex, as has previously been suggested for other oncofusion proteins,[32] and/or that FUS–ERG collaborates with other ETS factors.

To examine which other ETS factors might be involved in regulating ETS motif-containing binding sites, we performed a DNA pull-down experiment using a specific nucleotide sequence that contains the ETS consensus motif 5′-CCGGAAG-3′ (ETS bait) and a control sequence (Control bait) with a scrambled

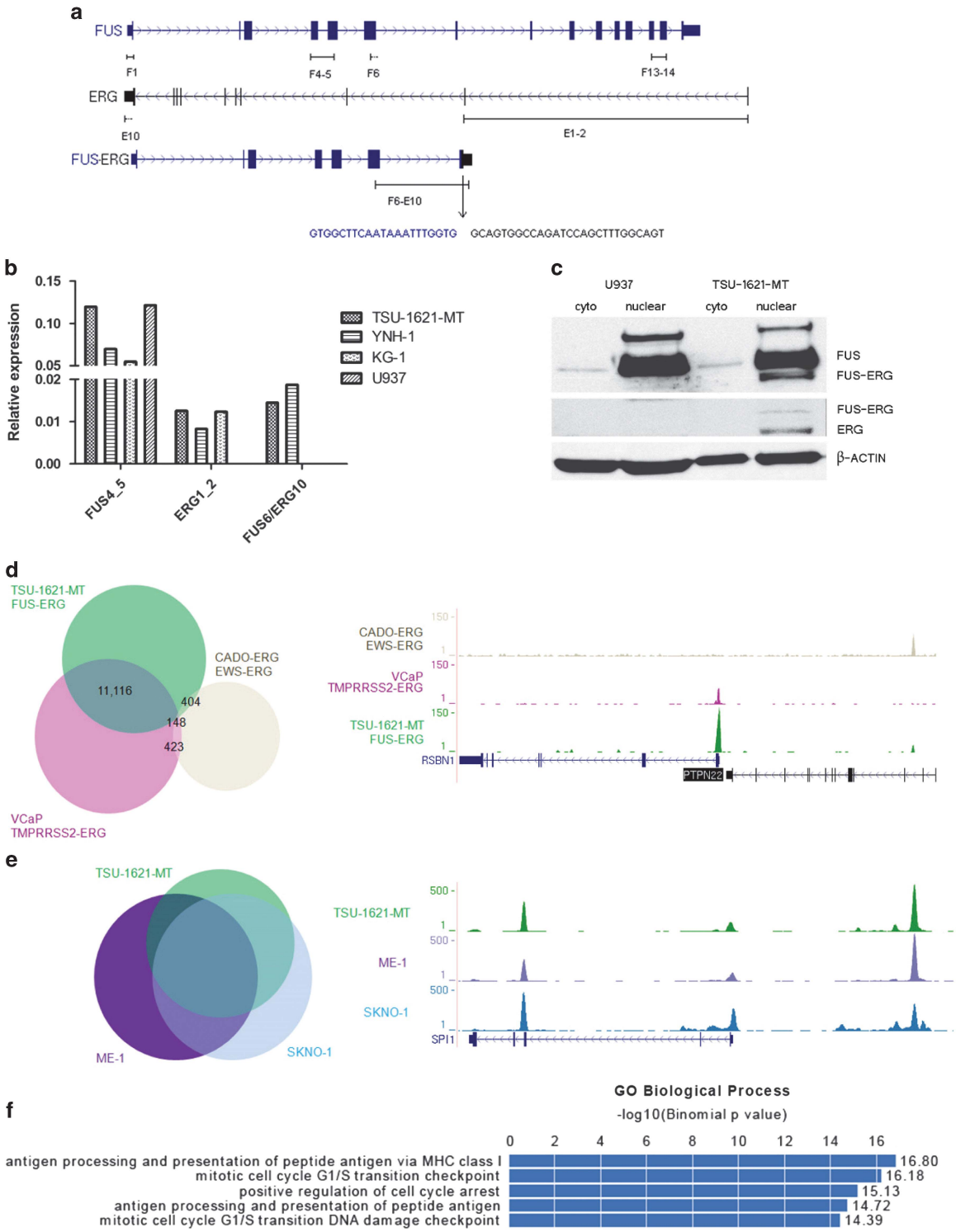

Figure 1. Aberrant ERG expression in cancer. (**a**) Schematic diagram of the organization of *FUS* (blue) and *ERG* (black) genes. Genomic organization of the *FUS–ERG* fusion gene at the chromosome translocation breakpoint. Boxes indicate exons; lines indicate introns. (**b**) Gene expression levels of *FUS* (exons 4–5), *ERG* (exons 1–2) and *FUS–ERG* (*FUS* exon 6–*ERG* exon 10) determined by quantitative real-time PCR (qPCR). The relative expression levels of the genes indicated (*x* axis) were assessed in the t(16;21) AML cells TSU-1621-MT and YNH-1 and in two control cell lines KG-1 and U937. (**c**) Western analysis of the cytoplasmic and nuclear fraction of U937 and TSU-1621-MT cells using antibodies recognizing FUS, ERG and a control β-actin antibody. (**d**) Venn diagram representing the overlap of ERG-binding sites in CADO-ERG, VCaP and TSU-1621-MT cells (left). ChIP-seq using ERG antibody. Overview of the *RSBN1* and *PTPN2* EWS–ERG, TMPRRSS2–ERG and FUS–ERG-binding sites (right). Brown represents the EWS–ERG ChIP-seq data; pink, the TMPRRSS2–ERG data and green the FUS–ERG data. (**e**) Venn diagram representing the overlap of ERG-binding sites in the AML cell lines TSU-1621-MT, ME-1 and SKNO-1 (left). ChIP-seq using ERG antibody. Overview of the *SPI1* ERG-binding sites in TSU-1621-MT, ME-1 and SKNO-1 cells (right). Green represents the TSU-1621-MT ChIP-seq data; purple, the ME-1 data and blue SKNO-1 data. (**f**) Bar chart showing the enrichment of biological process of FUS–ERG-binding sites in TSU-1621-MT cells (based on a single ontology-specific table from GREAT). The metric plotted is the binomial *P*-value. GO, gene ontology; MHC, major histocompatibility complex.

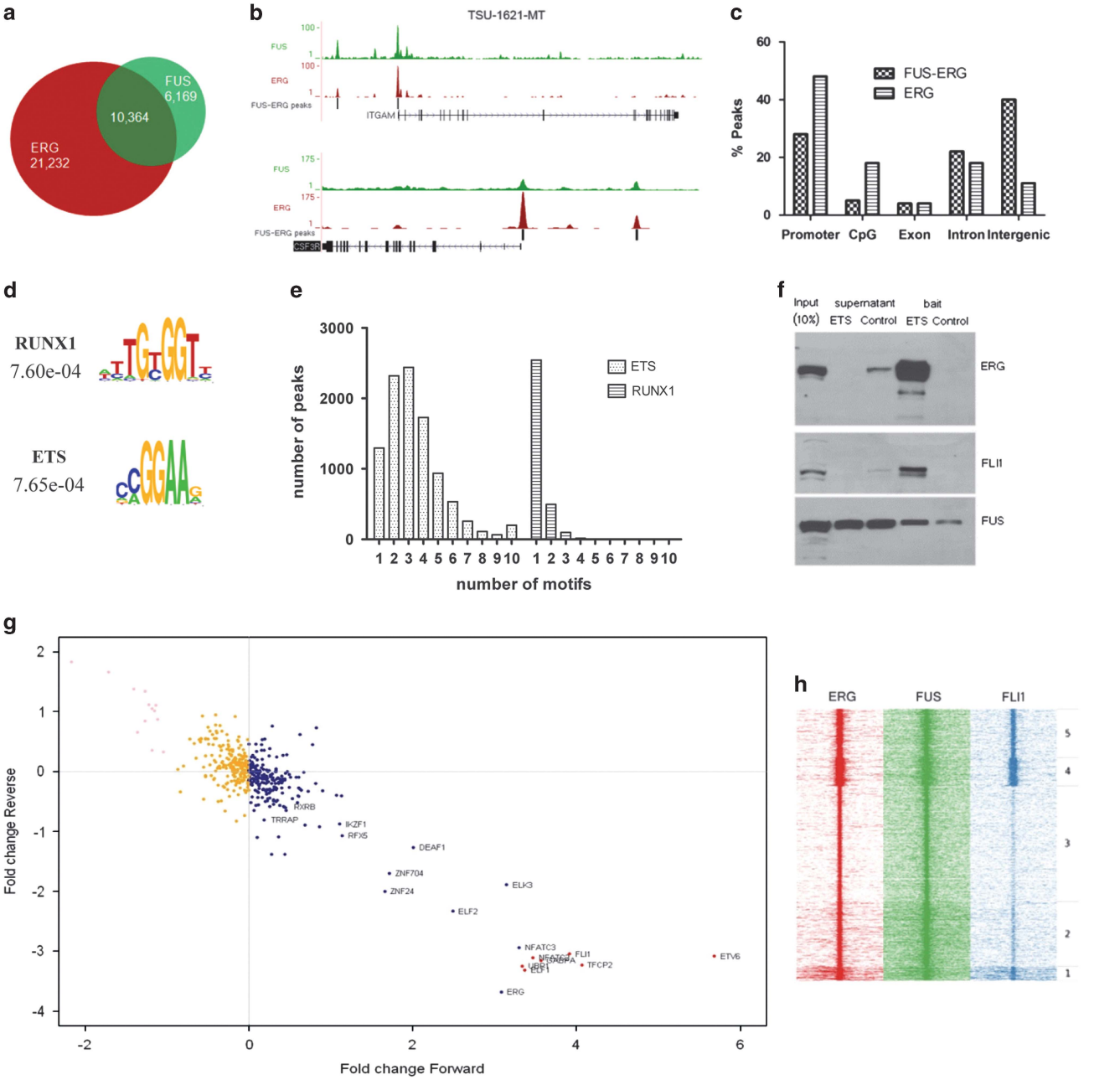

Figure 2. Genome-wide binding of FUS–ERG. (**a**) Venn diagram representing the overlap of FUS- and ERG-binding sites in TSU-1621-MT cells. (**b**) ChIP-seq using FUS and ERG antibodies. Overview of the *ITGAM* and *CSF3R* FUS- and ERG-binding sites in TSU-1621-MT cells. Green represents the FUS-binding-site data; red the ERG ChIP-seq data and black the FUS–ERG peaks in TSU-1621-MT cells. (**c**) Distribution of the FUS–ERG- and ERG-binding site locations relative to RefSeq genes. Locations of binding sites are divided in promoter (−500 bp to the transcription start site), non-promoter CpG island, exon, intron and intergenic (everything else). (**d**) Motif analysis of the FUS–ERG-binding sites. Overview of the resulted scores of ETS and RUNX1 core-binding motifs. (**e**) Number of FUS–ERG peaks that harbor a given number (indicated on the *x* axis) of ETS or RUNX1 motifs. (**f**) Western analysis of a DNA pull-down in TSU-1621-MT cells using ERG, FLI1 and FUS antibodies. ERG, FLI1 and FUS are more enriched in the pull-down with the ETS motif in comparison with the control. Specific binding to the oligo is further confirmed by ERG and FLI1 depletion in the supernatant that is left after incubation with the ETS oligo, but not with the Control oligo. (**g**) Scatter plot showing the result of a pull-down mass spectrometry experiment. Proteins are plotted by their dimethyl ratios in the forward (*x* axis) and reverse (*y* axis) SILAC experiment. ETS proteins and specific interactors of the ETS pull-down lie in the lower right quadrant. (**h**) Heat map displaying ERG and FLI1 tag densities at high-confidence FUS–ERG-binding sites.

ETS motif (Supplementary Table 3). The ETS bait motif used represents the consensus site for class I, IIa, IIb and IV ETS family members,[29] such as ERG, ELF1 and FLI1, whereas class III family members such as SPI1 bind a distinctive consensus motif 5′-G(A/G)GGAAG-3′. Western blot experiments confirmed that the ETS-motif-containing oligo efficiently pulls down ERG, as well as FUS–ERG from TSU-1621-MT cell lysates (Figure 2f). Specific binding to the oligo was further confirmed by ERG depletion in the supernatant that is left after incubation with the ETS oligo, but not with the Control oligo (Figure 2f).

Subsequently, the protein extracts derived from TSU-1621-MT cells incubated with oligonucleotides containing the ERG or a scrambled ERG motif were subjected to specific labeling methods with ‘heavy’ or ‘medium’ dimethyl labels, and analyzed by mass

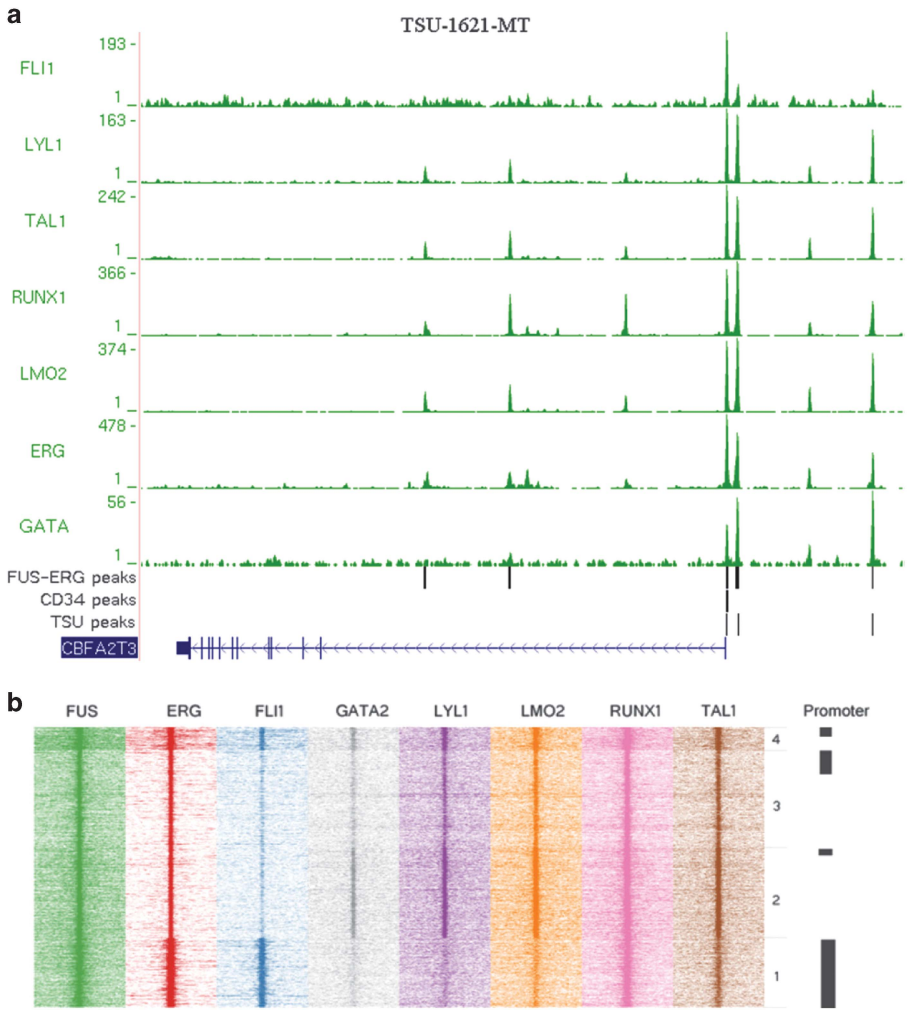

Figure 3. FUS–ERG binds genomic regions occupied by a heptad of transcription factors. (**a**) ChIP-seq using heptad (ERG, FLI1, GATA2, LYL1, LMO2, RUNX1 and TAL1) antibodies. Overview of the *CBFA2T3* heptad-binding sites in TSU-1621-MT cells. 'FUS–ERG peaks' represent regions occupied by FUS and ERG, 'CD34+ peaks' represent heptad-binding sites in CD34+ cells and 'TSU peaks' represent heptad peaks in TSU-1621-MT cells. (**b**) Heat map displaying ERG, FLI1, GATA2, LYL1, LMO2, RUNX1 and TAL1 tag densities at high-confidence FUS–ERG-binding sites.

spectrometry[33] (see Supplementary Materials and methods). As expected, specifically ETS family members of the I, IIa, IIb and IV classes, but not SPI1, were enriched in the ETS motif pull-down (Figure 2g). Unfortunately, peptides recognizing the N terminus of FUS (present in WT FUS and in FUS–ERG) were not found, likely due to the inability of trypsin to digest the FUS glycine-rich regions. Interestingly, the ratio of Control vs ETS pull-down peptides was higher for FUS C-terminal peptides, representing WT FUS, suggesting WT FUS is underrepresented at genomic regions harboring ETS consensus sequences. As our ChIP-seq results using an N-terminal antibody indicate enrichment of FUS at ETS-containing-binding sites, this signal is likely due to the fusion of FUS and ERG.

To confirm the interactions of FLI1 with the ETS-motif-containing DNA fragment, we used an antibody recognizing FLI1 in western analysis after pull-down, as well as in ChIP-seq. This revealed specific FLI1 binding to the ETS-containing DNA fragment (Figure 2f), as well as increased occupancy of FLI1 at FUS–ERG-binding sites (Figure 2h), corroborating the pull-down results.

FUS–ERG does not interfere with assembly of a hematopoietic transcription factor complex

Both ERG and FLI1 have been suggested to function in a heptad of proteins,[34–36] which is central to proper expression of genes involved in maintaining a stem cell hematopoietic phenotype. RNA-seq analysis using TSU-1621-MT cells revealed that all these seven heptad transcription factors (GATA2/FLI1/RUNX1/TAL1/LYL1/LMO2/ERG) are expressed in this cell type, suggesting that also in the context of FUS–ERG the heptad can potentially assemble. To examine whether the heptad is present or whether assembly of the heptad is interfered due to the FUS–ERG fusion, we performed ChIP-seq for all the heptad factors in TSU-1621-MT cells (Figure 3a). Analyzing the binding data revealed that in TSU-1621-MT cells heptad complexes were present, and that the majority of the heptad-binding sites were occupied by FUS–ERG, suggesting that the FUS moiety does not interfere with TF complex assembly (Figure 3b). We further characterized the distribution of binding events across FUS–ERG/heptad-occupied genomic features and identified four clusters that could be distinguished on different levels of FLI1, GATA2 and LYL1. Clusters 2 and 3 represent intergenic regions with relatively low FLI1 levels, and are functionally enriched for abnormal hematopoiesis, apoptosis signaling and myeloid cell differentiation. Cluster 4 represents promoter regions with higher levels of FLI1 and LYL1 and is functionally enriched for cell proliferation, myeloid differentiation and immune response. In contrast, cluster 1, which is linked to promoter regions, is enriched for transcriptional coupled events and represents regions strongly bound by ERG,

FLI1, RUNX1 and TAL1. Together these results suggest that FUS–ERG does not interfere with heptad formation, but that depending on the genomic context, occupancy strength of heptad components can vary.

Next, we compared the heptad occupancy in the TSU-1621-MT cells with available data from non-leukemic CD34$^+$ cells,[36] which represent a normal hematopoietic cell population. We found enrichment of heptad components in CD34$^+$ cells at some of our FUS–ERG-binding sites, for example, HHEX, LAPTM5 and CBFA2T3 genes were bound by all seven TFs in both cell types (Supplementary Figures 5A and B). Together these results suggest that the heptad distribution in TSU cells resembles only part of the heptad signature in CD34$^+$ cells.

FUS–ERG modulates the ATRA response

FUS/TLS has been reported to interact with RXR,[10] and also our mass spectrometry analysis revealed approximately twofold enrichment of RXR (RXRβ) in the ETS-motif-containing DNA pull-down (Figure 2g). To examine whether FUS–ERG binds similar genomic regions as RXR, we performed ChIP-seq using an RXR antibody (recognizing RXRα, RXRβ and RXRγ). This analysis revealed enrichment of RXR at high-confidence FUS–ERG-binding sites (Figures 4a and b), although at varying strength. As RXR is acting in heterodimeric complexes, we wondered whether another nuclear receptor could be present interacting with RXR. We found a variety of other nuclear receptors expressed in normal TSU-1621-MT cells, of which RARA was one of the highest nuclear receptors expressed known to form a heterodimer with RXR (Figure 4c). Moreover, as RARA is a common fusion partner in acute promyelocytic leukemias (APLs),[37] another subsets of AMLs, we wondered whether RARA could be present in the FUS–ERG/RXR complex.

To answer this question, we performed ChIP-seq using a RARA antibody. Quantitation of RARA tag densities at FUS–ERG peaks revealed enrichment of RARA at FUS–ERG-binding sites (Figures 4a and b), suggesting that FUS–ERG might be involved in regulating retinoic acid signaling in t(16;21) AMLs.

A variety of AML cells have been shown to be responsive to ATRA treatment, in particular AMLs harboring a translocation involving RARA. No studies so far have considered patients with t(16;21) (p11;q22) translocations as possible candidates for retinoic acid treatment. As our findings show that RARA:RXR might function as a partner of FUS–ERG, we wondered whether these AML cells would be responsive to ATRA treatment. Therefore, TSU-1621-MT cells were exposed to different concentrations of ATRA during 4 days. The rate of cell growth for the TSU-1621-MT cells was calculated as 0.7 times/day. After 4 days, the number of viable cells had increased 2.5-fold (Figure 5a). This slow increase of cell number was halted by the presence of ATRA, as evidenced by reduced viability (Figure 5a) and differentiation of the cells (5–8% of the total living cells per day attached to the plate) into granulocytes (Figure 5b).

In APL, ATRA treatment was shown to increase histone acetylation levels at PML–RARA-binding sites. To examine whether histone acetylation is changed at FUS–ERG-binding sites, we performed ChIP-seq analysis using antibodies recognizing histone H3K9K14 acetylation. After ATRA treatment, increased levels of H3 acetylation were observed at nearly all binding sites (Figure 5c), suggesting a role for the fusion protein in maintaining a less-active chromatin structure.

To examine which genes are differentially expressed upon ATRA treatment, we exposed TSU-1621-MT cells for 24 h to 1 μM ATRA

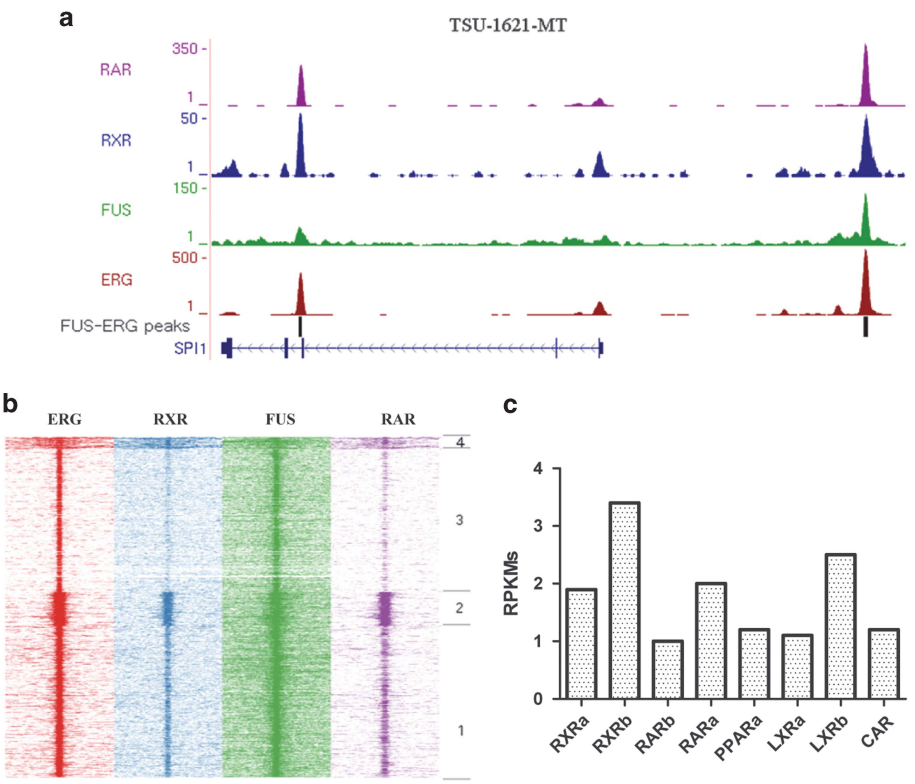

Figure 4. FUS–ERG targets RXR:RARA-binding sites. (**a**) ChIP-seq using RARA, RXR, FUS and ERG antibodies. Overview of the SPI1-binding sites in TSU-1621-MT cells. Pink represents RARA data; blue represents the RXR data; green represents the FUS data; red, the ERG ChIP-seq data and black the FUS–ERG peaks identified in TSU-1621-MT cells. (**b**) Heat map displaying ERG, RXR, FUS and RARA tag densities at high-confidence FUS–ERG-binding sites. (**c**) Barplot showing the expression levels (RPKMs) of nuclear receptors in the RNA-seq data.

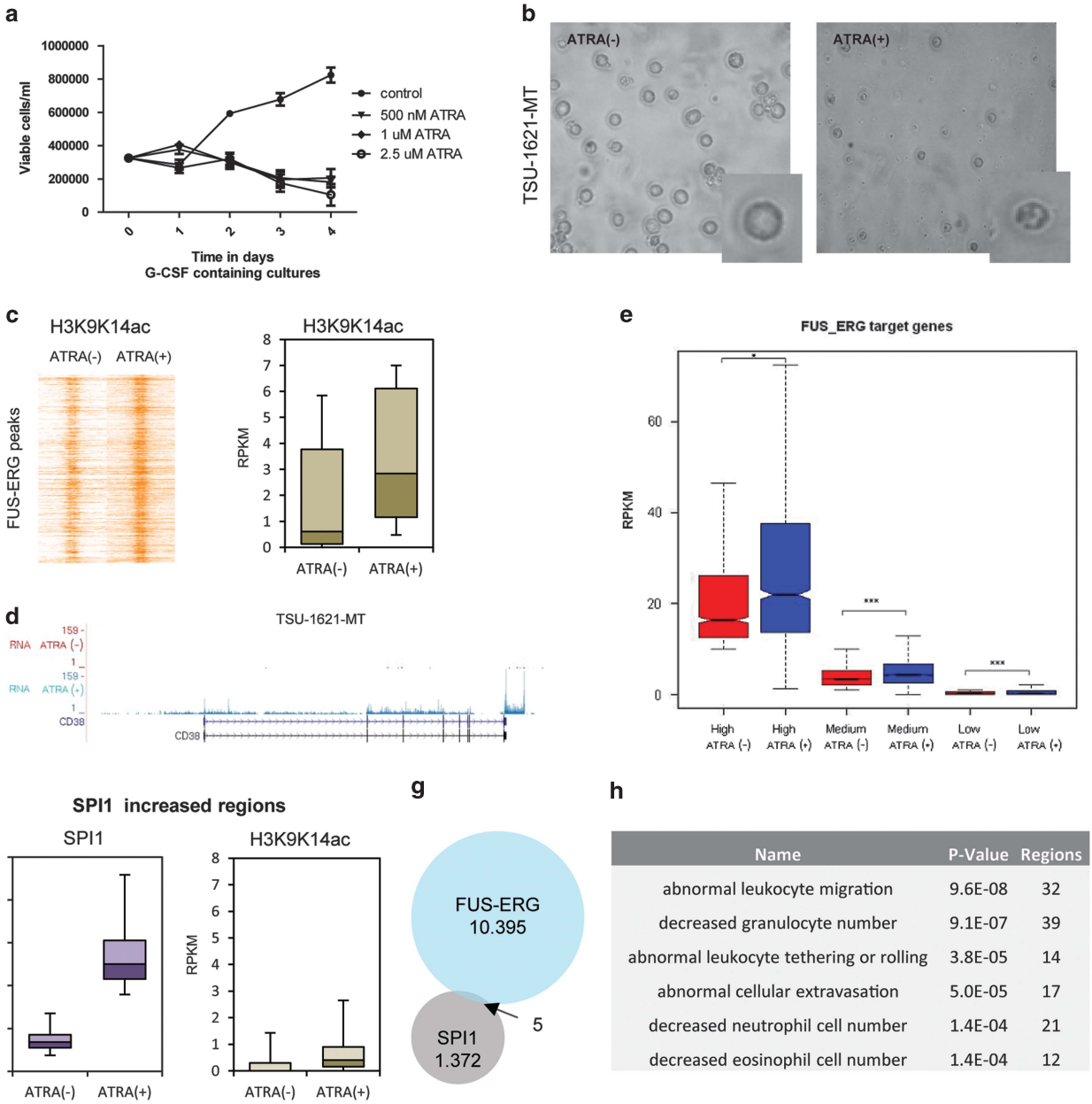

Figure 5. ATRA treatment of t(16;21) AML cells reduces viability and increases expression of FUS–ERG target genes. (**a**) Viability curves in TSU-1621-MT cells ($n = 3$) exposed to increasing concentrations of ATRA over time. (**b**) Cell pictures of TSU-1621-MT cells before and after ATRA treatment. The inset zooms in on one of the cells. (**c**) Heat map (left) and box plot (right) displaying H3K9K14ac densities at high-confidence FUS–ERG-binding sites before and after treatment of TSU-1621-MT cells with ATRA. (**d**) Overview of RNA-seq data in TSU-1621-MT cells treated or untreated with ATRA at the CD38 genomic region. RNA tracks are represented in red for untreated cells and in blue for cells after 24 h of ATRA treatment. (**e**) Box plot showing RPKM values of FUS–ERG-target genes before (red) and after (blue) ATRA treatment. FUS–ERG-target genes are divided in three groups, high (>10 RPKMs), medium (1 < RPKMs < 10) and low (RPKMs < 1). $^{*}P < 0.05$, $^{***}P < 0.0005$. (**f**) Box plot displaying SPI1 and H3K9K14ac densities at ATRA increased SPI1-binding sites before and after treatment of TSU-1621-MT cells with ATRA. (**g**) Venn diagram representing the overlap of FUS–ERG and ATRA increased SPI1-binding sites. (**h**) Functional annotation (mouse knockout phenotype) of genes associated with increased SPI1-binding sites.

and performed RNA-seq analysis. Gene expression levels from control and treated cells were estimated by counting the number of reads mapping to constitutive exons for each gene and determining RPKM values (reads per kilobase of exon model per million uniquely mapped reads).

Initial analysis of CD markers revealed significant increased RPKM values for the differentiation marker CD38 compared with untreated cells (Figure 5d; Supplementary Tables 5 and 6). Other CD markers shown to be lower expressed after ATRA treatment (log ratio < -1) were the progenitor markers HLA-DR, CD34 and CD44, whereas granulocytic markers such as CD13, CD15, CD11b, CD18 and MPO were higher expressed. As also increased expression of other granulocytic markers including HIC1, ASB2 and NCF1 was observed after treatment, these results suggest differentiation of ATRA-treated TSU-1621-MT cells toward the granulocyte lineage.

To examine the effect of ATRA treatment on FUS–ERG target genes, we assigned FUS–ERG-binding sites to the closest gene and analyzed gene expression. This revealed that FUS–ERG target genes are expressed at different level with 11% of genes

expressed at a high level (RPKM > 10), 59% moderately expressed (1 < RPKM < 10) and 30% low expressed (RPKM < 1) (Figure 5e, red boxes). RT–qPCR of a selection of genes from each of these three groups confirmed their relative expression results in both TSU1621-MT as well as YNH-1 cells (Supplementary Figure 6). Upon ATRA treatment, we observed increased expression for a majority of FUS–ERG target genes (68%; Figure 5e, blue boxes), suggesting FUS–ERG functions as a transcriptional repressor of genes that are part of the ATRA signaling pathway.

Our results identified FUS–ERG binding at the third intron of SPI1 (Figure 4a), a key regulator of hematopoietic differentiation. It is characterized by the presence of direct repeat motifs, which represent canonical RARA:RXR-binding sites (Supplementary Figure 7A), as well as the consensus binding sequence for ETS factors (such as ERG). This region has previously been associated with repression of SPI1 transcription,[38] which can in APLs be relieved after treatment with ATRA.[37] In line with the suggestion that FUS–ERG functions as a repressor of transcription, also in ATRA-treated TSU-1621-MT cells SPI1 expression is increased (Supplementary Table 6). SPI1 and ERG are both members of the ETS family of transcription factors. We wondered whether SPI1 could alter the FUS–ERG-repressed gene program through increased binding activity at FUS–ERG target genes after ATRA treatment. However, ChIP-seq results of SPI1 binding before and after ATRA treatment of TSU-1621-MT cells revealed no differences in binding-site occupancy at FUS–ERG-binding sites (Supplementary Figure 7B). Still, using a threefold cutoff we identified 1377 genomic regions were SPI1 binding is increased (Figure 5f, left). As expected, these regions do not overlap with FUS–ERG-binding sites and represent sites of no/low histone acetylation, which is increased upon binding of SPI1 (Figure 5f, right; Figure 5g). Interestingly, these regions are associated with genes that, upon knockout in mice, are associated with granulocyte abnormalities (Figure 5h), suggesting that activation of these regions is required for normal granulopoiesis.

Together these results suggest that FUS–ERG acts as a repressor of SPI1, preventing it from activating a granulocytic differentiation program.

ATRA treatment induces a FUS–ERG/ERG switch at enhancer regions

To examine the effect of ATRA treatment on FUS–ERG binding, we performed ChIP-seq using FUS and ERG antibodies in ATRA-treated TSU cells. In addition, we included RNAPII occupancy after treatment, allowing to validate alterations in transcriptional activity. K-means clustering distinguished five groups of FUS–ERG-binding sites (Figures 6a and b). Whereas clusters 1, 3 and 4 were characterized by increases in ERG and lowered FUS occupancy, clusters 2 and 5 showed reduced FUS and ERG levels, suggesting that FUS–ERG binding is lost and that at a subset of regions (clusters 1, 3 and 4) ERG binding is gained. Interestingly, sites where ERG occupancy is increased are mostly non-promoter (~85%) (clusters 1, 3 and 4) and show increased levels of RNAPII, suggesting these are enhancers activated upon ATRA treatment (Figure 6b; Supplementary Figure 8). Functional analysis of these three clusters revealed a clear enrichment of genes down-regulated in AML1–ETO and PML–RARα leukemic translocations, suggesting that these represent a set of regions commonly targeted in different subtypes of AML. Additional comparison with AML1–ETO and PML–RARα-binding regions, 2754 and 2721 peaks, respectively,[20,37] pointed out that indeed, 50–60% of regions overlapped (Supplementary Table 7).

In contrast to clusters 1, 3 and 4, clusters 2 and 5, which represent mostly promoter regions (~83%), showed enrichment for mRNA metabolism, mRNA splicing, cell cycle check points and gene expression. These two clusters show loss of RNAPII occupancy upon ATRA treatment, likely representing a switch from a poised RNAPII to a transcriptional active molecule.

FUS–ERG silencing results in cell death

To examine the molecular targeting of the FUS–ERG oncofusion protein in TSU-1621-MT cells, we generated a small-hairpin RNA (shRNA) construct targeting the fusion point sequence of FUS–ERG under the control of a tetracycline-regulated promoter (FH1t-UTG). FUS–ERG-silenced TSU-1621-MT cells (Supplementary Figure 9) resulted in cell death and decreased proliferation (Figure 7a), suggesting FUS–ERG is needed to maintain the full leukemogenic potential of these cells.

To examine the effect of FUS–ERG knockdown on target gene expression, we performed RNA-seq analysis. We identified 1833 FUS–ERG target genes, such as CTNNB1 and IL1B (Supplementary Figure 10) that were differentially expressed. Among these genes, 1149 were upregulated and 684 were downregulated by at least twofold (Supplementary Table 8), suggesting FUS–ERG is involved in gene repression, but can also activate particular gene sets. In agreement with the knockdown-induced cell death, we found increased expression of genes inducing apoptosis, such as *CASP10*, *ATM*, *SAMD3*, *BMF* and *FAF1*, whereas anti-apoptotic genes such as *BCL-2*, *GADD45B*, *IL1B* and *IL2RA* were downregulated.

Finally, we integrated the knockdown analysis with the ATRA-induced differentiation results to identify the key ATRA-responsive genes regulated by FUS–ERG. A scatter plot (Figure 7b) showing the log2 ratios of both the shRNA knockdown experiment (*x* axis; induced/non-induced) and the ATRA-differentiation experiment (*y* axis; ATRA treated/non-treated) revealed 138 FUS–ERG target genes higher expressed after FUS–ERG knockdown or after ATRA treatment. This set is enriched for genes involved in myeloid differentiation (Figure 7b), suggesting FUS–ERG has a role in repressing this particular gene set from becoming activated by ATRA. In contrast, among the common 76 downregulated genes, enrichment for immune response, anti-apoptosis and cytokine–cytokine receptor interaction pathways were found.

Together our results suggest that FUS–ERG acts in part as a transcriptional repressor of the retinoic acid signaling pathway for a subset of target genes. It acts in the context of other master hematopoietic transcription factors, as well as RARA:RXR to inhibit genes that can drive myeloid differentiation. Both ATRA treatment and FUS–ERG knockdown can alleviate this repression and induce expression of this set of target genes (Figure 7c).

DISCUSSION

AMLs harboring t(16;21)(p11;q22) express the oncofusion protein FUS–ERG. Expression of this fusion protein in normal human myeloid progenitors has been shown to result in a block in development at the promyelocytic stage,[39] an arrest in erythroid and myeloid differentiation and an increase in proliferation and self-renewal capacity of human myeloid progenitors.[39] However, these transduction experiments can only partially recapitulate the disease state.[40] In this study, we describe for the first time the molecular mechanisms underlying the actions of the FUS–ERG oncofusion in AML at a genome-wide level in patient-derived cell line models. We found that this oncofusion is expressed at similar levels as WT ERG, and might interfere with normal ETS factor regulation. To identify FUS–ERG binding, we used two antibodies specifically recognizing the N terminus of FUS and the C terminus of ERG. We identified a set of 10 364 genomic regions, mainly intergenic and thus representing putative enhancer regions, to which FUS–ERG binds. We discovered that the oncofusion protein occupies genomic regions bound by ERG, RUNX1, FLI1, GATA2, LMO2, LYL1 and TAL1/SCL, which together form a heptad of transcription factors associated with stem cell programs and clinical outcome in AML, suggesting the expression

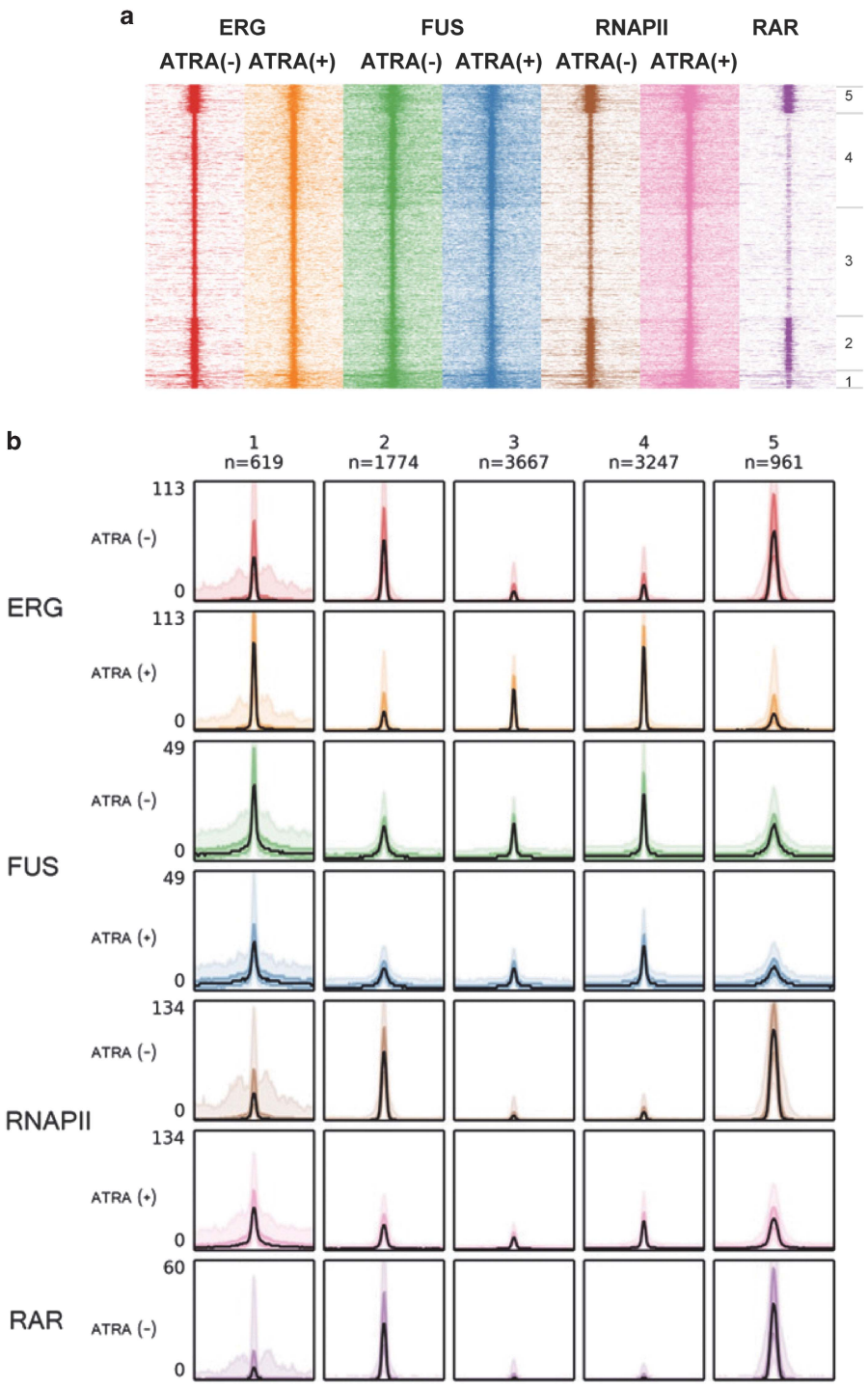

Figure 6. ERG and RNAPII changes at FUS–ERG-binding sites. (**a**) Heat map displaying ERG, FUS, RNAPII and RARA tag densities in untreated or ATRA-treated TSU-1621-MT cells at high-confidence FUS–ERG-binding sites. (**b**) Density plots of K-means-clustered ERG, FUS, RNAPII and RARA tag densities in untreated or ATRA-treated TSU-1621-MT cells at high-confidence FUS–ERG-binding sites. *n* represents the number of binding sites per cluster.

of FUS–ERG might interfere with the activity but not the assembly of this heptad.

In addition, we identified binding of the nuclear receptor heterodimer RARA:RXR to FUS–ERG-occupied genomic regions, suggesting the oncofusion protein might be involved in modulating the retinoic acid response. Treatment of t(16;21) cells with all-*trans* retinoic acid resulted in cell differentiation, as exemplified by increased expression of the myeloid differentiation markers CD11b and CD38.[41,42] Prolonged treatment with ATRA resulted in apoptosis consistent with the onset of post-differentiation cell death. Together these results suggest that ATRA triggers differentiation and thereby stops self-renewal in t(16;21) AML cells. Thus far, only APLs are unique among leukemias due to their sensitivity to ATRA.[43] However, our results would suggest that also for t(16;21) AMLs ATRA treatment might provide an entry point for eradicating leukemic cells.

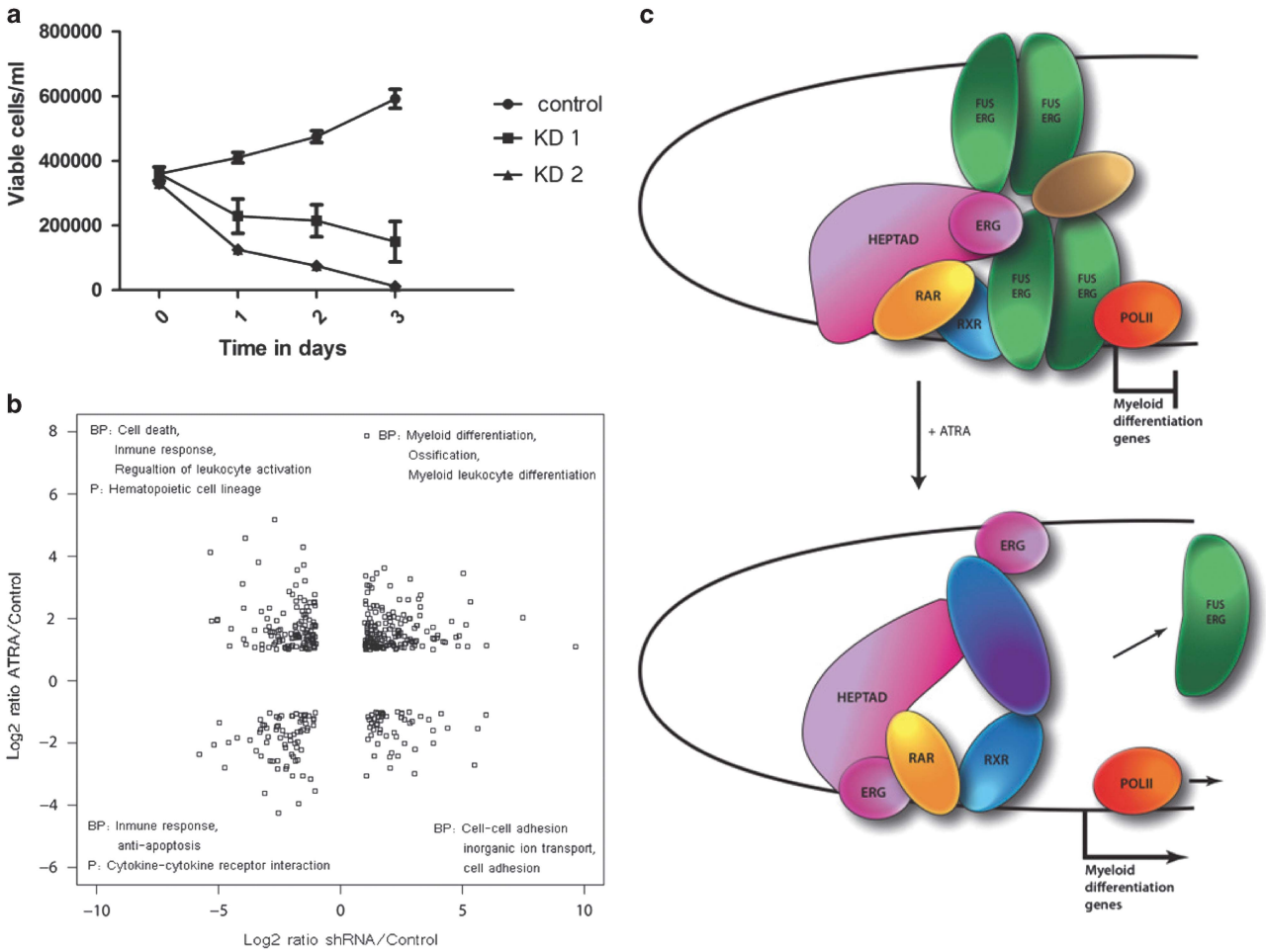

Figure 7. FUS–ERG knockdown alters the t(16;21) AML gene expression program. (**a**) Viability curves in TSU-1621-MT cells in samples with 23% knockdown (KD1) or 40% knockdown (KD2) of FUS–ERG over a period of 3 days. (**b**) Scatter plot of RPKM values (log2) for FUS–ERG-regulated genes. The *y* axis represents expression of ATRA-treated genes versus control; the *x* axis represents expression of genes when induced with shRNA versus not induced. Each quadrant shows the gene enrichment for biological processes (BPs) and pathways (Ps). (**c**) Schematic model for the suggested actions of FUS–ERG in t(16;21) cells before and after ATRA treatment. Before treatment, FUS–ERG binds as an oligomer to promoter and intergenic regions together with a heptad of transcription factors, as well as RARA:RXR and RNAPII. After ATRA treatment, FUS–ERG is lost from the complex allowing RNAPII to transcribe genes involved in myeloid differentiation.

Our genome-wide profiling revealed that upon ATRA treatment FUS–ERG binding is lost at enhancers and promoters, correlating with increased ERG binding at enhancers and loss of RNAPII binding at promoters. RNAPII loss at promoters likely reflects transcriptional initiation corroborating the RNA-seq analysis that revealed increased transcription of a majority of FUS–ERG target genes. Together these results suggest FUS–ERG might act as a transcriptional repressor.

To further test this, we performed knockdown of FUS–ERG in t(16;21) cells and could show that loss of the oncofusion protein results in higher expression of a subset of 138 genes that are also higher expressed after ATRA treatment. Interestingly, functional analysis of this gene set revealed enrichment for myeloid-differentiation programs, corroborating at the gene level the FUS–ERG-imposed block of retinoic acid-induced differentiation.

The repressive activities of FUS–ERG toward myeloid-differentiation genes including master regulators of hematopoiesis, such as *SPI1*, *GATA2*, *GFI1*, *JUNB* or *JUNC*, mimic the molecular effects previously reported for other oncofusion proteins such as AML1–ETO[20] and PML–RARA,[37,44] which target many of the same genes as FUS–ERG. Both AML1–ETO and PML–RARA have been shown to multimerize and recruit histone deacetylase activities in order to repress target gene transcription.[45–49] As FUS–ERG-binding sites harbor multiple ETS consensus sequences and the oncofusion protein through its FUS domain might also have oligomerization capacity,[50] it is tempting to speculate that FUS–ERG might use a similar mechanism to inhibit transcription.

Together our results reveal that FUS–ERG has a key role in t(16;21) AMLs, through aberrant regulation of the ATRA response and inhibiting differentiation along the myeloid lineage.

MATERIALS AND METHODS

Cell culture

TSU-1621-MT cells (DSMZ) were cultured in RPMI 1640 supplemented with 10% fetal calf serum, 10 ng/ml of granulocyte colony-stimulating factor and incubated at 37 °C and in 5% CO_2.[51] YNH-1 cells (DSMZ) were cultured in RPMI 1640 supplemented with 10% fetal calf serum, 10 ng/ml of IL-3 or 10 ng/ml of granulocyte colony-stimulating factor and incubated at 37 °C and 5% CO_2.[5,8] Both cell lines were mycoplasma free.

Chromatin immunoprecipitation (ChIP)

Chromatin was harvested as described.[52] ChIPs were performed using specific antibodies to ERG, FLI1, RXRα, SPI1, TAL1, LYL1, GATA2, LMO2 (Santa Cruz, Dallas, TX, USA), RARA, H3K9K14ac, RNAPII (Diagenode, Liege, Belgium), FLI1, RUNX1 (Abcam, Cambridge, UK) and FUS (lot. A300-302 A-1

that detects the N-terminal domain, Bethyl) and analyzed by qPCR or ChIP-seq (see also Supplementary Information). Primers for qPCR are described in Supplementary Table 1. Relative occupancy was calculated as fold over background, for which the second exon of the *Myoglobin* gene or the promoter of the *H2B* gene was used.

Illumina high-throughput sequencing

End repair was performed using the precipitated DNA of ~6 million cells (3–4 pooled biological replicas) using Klenow and T4 PNK. A 3′-protruding A base was generated using Taq polymerase, and adapters were ligated. The DNA was loaded on gel and a band corresponding to ~300 bp (ChIP fragment+adapters) was excised. The DNA was isolated, amplified by PCR and used for cluster generation on the Genome analyzer (Illumina, San Diego, CA, USA) and HiSeq 2000 (Illumina). The 50-bp tags were mapped to the human genome HG18 using the eland program allowing 1 mismatch or Burrows-Wheeler Aligner.[53] For each base pair in the genome, the number of overlapping sequence reads was determined and averaged over a 10-bp window and visualized in the UCSC genome browser (http://genome.ucsc.edu). A list of the ChIP-seq profiles analyzed in this study can be found in Supplementary Table 2. For processing and manipulation of SAM/BAM files, SAM tools[54] were used. All ChIP-seq data can be downloaded from Gene Expression Omnibus accession number GSE60477.

CONFLICT OF INTEREST

The authors declare no conflict of interest.

ACKNOWLEDGEMENTS

This work was supported by the EU (BLUEPRINT-282510), the Dutch Cancer Foundation (KWF KUN 2009-4527 and KUN 2011-4937) and the Netherlands Organization for Scientific Research (NWO-VIDI to JHAM). Database accession: All ChIP-seq and RNA-seq data can be downloaded from the NCBI Gene Expression Omnibus (GEO) (http://www.ncbi.nlm.nih.gov/geo/) under accession number GSE60477.

REFERENCES

1 Sharrocks AD, Brown AL, Ling Y, Yates PR. The ETS-domain transcription factor family. *Int J Biochem Cell Biol* 1997; **29**: 1371–1387.
2 Salek-Ardakani S, Smooha G, de Boer J, Sebire NJ, Morrow M, Rainis L *et al.* ERG is a megakaryocytic oncogene. *Cancer Res* 2009; **69**: 4665–4673.
3 Tomlins SA, Rhodes DR, Perner S, Dhanasekaran SM, Mehra R, Sun X-W *et al.* Recurrent fusion of TMPRSS2 and ETS transcription factor genes in prostate cancer. *Science* 2005; **310**: 644–648.
4 Sorensen PHB, Lessnick SL, Lopez-Terrada D, Liu XF, Triche TJ, Denny CT. A second Ewing's sarcoma translocation, t(21;22), fuses the EWS gene to another ETS – family transcription factor, ERG-EWS gene to another ETS – family transcription factor, ERG. *Nat Genet* 1994; **6**: 146–151.
5 Yamamoto K, Hamaguchi H, Nagata K, Kobayashi M, Tanimoto F, Taniwaki M. Establishment of a novel human acute myeloblastic leukemia cell line (YNH-1) with t(16;21), t(1;16) and 12q13 translocations. *Leukemia* 1997; **11**: 599–608.
6 Prasad DD, Ouchida M, Lee L, Rao VN, Reddy ES. TLS/FUS fusion domain of TLS/FUS-erg chimeric protein resulting from the t(16;21) chromosomal translocation in human myeloid leukemia functions as a transcriptional activation domain. *Oncogene* 1994; **9**: 3717–3729.
7 Crozat A, Aman P, Mandahl N, Ron D. Fusion of CHOP to a novel RNA-binding protein in human myxoid liposarcoma. *Nature* 1993; **363**: 640–644.
8 Zou J, Ichikawa H, Blackburn ML, Hu H-M, Zielinska-Kwiatkowska A, Mei Q *et al.* The oncogenic TLS-ERG fusion protein exerts different effects in hematopoietic cells and fibroblasts. *Mol Cell Biol* 2005; **25**: 6235–6246.
9 Yang L, Embree LJ, Hickstein DD. TLS-ERG leukemia fusion protein inhibits RNA splicing mediated by serine-arginine proteins. *Mol Cell Biol* 2000; **20**: 3345–3354.
10 Powers CA, Mathur M, Raaka BM, Ron D, Samuels HH. (TLS translocated-in-liposarcoma) is a high-affinity interactor for steroid, thyroid hormone, and retinoid receptors. *Mol Endocrinol* 1998; **12**: 4–18.
11 Zinszner H, Immanuel D, Yin Y, Liang F-X, Ron D. A topogenic role for the oncogenic N-terminus of TLS: nucleolar localization when transcription is inhibited. *Oncogene* 1997; **14**: 451–461.
12 Zinszner H, Sok J, Immanuel D, Yin Y, Ron D. TLS (FUS) binds RNA in vivo and engages in nucleo-cytoplasmic shuttling. *J Cell Sci* 1997; **110**: 1741–1750.
13 Delva L, Gallais I, Guillouf C, Denis N, Orvain C, Moreau-Gachelin F. Multiple functional domains of the oncoproteins Spi-1//PU.1 and TLS are involved in their opposite splicing effects in erythroleukemic cells. *Oncogene* 2004; **23**: 4389–4399.
14 Hallier M, Lerga A, Barnache S, Tavitian A, Moreau-Gachelin F. The transcription factor Spi-1/PU.1 interacts with the potential splicing factor TLS. *J Biol Chem* 1998; **273**: 4838–4842.
15 Mills KI, Walsh V, Gilkes AF, Sweeney MC, Mirza T, Woodgate LJ *et al.* High FUS/TLS expression in acute myeloid leukaemia samples. *Br J Haematol* 2000; **108**: 316–321.
16 Walsby EJ, Gilkes AF, Tonks A, Darley RL, Mills KI. FUS expression alters the differentiation response to all-trans retinoic acid in NB4 and NB4R2 cells. *Br J Haematol* 2007; **139**: 94–97.
17 Hicks GG, Singh N, Nashabi A, Mai S, Bozek G, Klewes L *et al.* Fus deficiency in mice results in defective B-lymphocyte development and activation, high levels of chromosomal instability and perinatal death. *Nat Genet* 2000; **24**: 175–179.
18 Sugawara T, Oguro H, Negishi M, Morita Y, Ichikawa H, Iseki T *et al.* FET family proto-oncogene Fus contributes to self-renewal of hematopoietic stem cells. *Exp Hematol* 2010; **38**: 696–706.
19 Lian Z, Wang L, Yamaga S, Bonds W, Beazer-Barclay Y, Kluger Y *et al.* Genomic and proteomic analysis of the myeloid differentiation program. *Blood* 2001; **98**: 513–524.
20 Martens JHA, Mandoli A, Simmer F, Wierenga B-J, Saeed S, Singh AA *et al.* ERG and FLI1 binding sites demarcate targets for aberrant epigenetic regulation by AML1-ETO in acute myeloid leukemia. *Blood* 2012; **120**: 4038–4048.
21 Bock J, Mochmann LH, Schlee C, Farhadi-Sartangi N, Gölner S, Müller-Tidow C *et al.* ERG transcriptional networks in primary acute leukemia cells implicate a role for ERG in deregulated kinase signaling. *PLoS One* 2013; **8**: e52872.
22 Ng AP, Loughran SJ, Metcalf D, Hyland CD, de Graaf CA, Hu Y *et al.* Erg is required for self-renewal of hematopoietic stem cells during stress hematopoiesis in mice. *Blood* 2011; **118**: 2454–2461.
23 Lacadie SA, Zon LI. The ERGonomics of hematopoietic stem cell self-renewal. *Genes Dev* 2011; **25**: 289–293.
24 Loughran SJ, Kruse EA, Hacking DF, de Graaf CA, Hyland CD, Willson TA *et al.* The transcription factor Erg is essential for definitive hematopoiesis and the function of adult hematopoietic stem cells. *Nat Immunol* 2008; **9**: 810–819.
25 Goldberg L, Tijssen MR, Birger Y, Hannah RL, Kinston SJ, Schütte J *et al.* Genome-scale expression and transcription factor binding profiles reveal therapeutic targets in transgenic ERG myeloid leukemia. *Blood* 2013; **122**: 2694–2703.
26 Kong X-T, Ida K, Ichikawa H, Shimizu K, Ohki M, Maseki N *et al.* Consistent detection of TLS/FUS-ERG chimeric transcripts in acute myeloid leukemia with t(16; 21)(p11; q22) and identification of a novel transcript. *Blood* 1997; **90**: 1192–1199.
27 Winnes M, Lissbrant E, Damber J, Stenman G. Molecular genetic analyses of the TMPRSS2-ERG and TMPRSS2-ETV1 gene fusions in 50 cases of prostate cancer. *Oncol Rep* 2007; **17**: 1033–1036.
28 Wei G-H, Badis G, Berger MF, Kivioja T, Palin K, Enge M *et al.* Genome-wide analysis of ETS-family DNA-binding in vitro and in vivo. *EMBO J* 2010; **29**: 2147–2160.
29 Yu J, Yu J, Mani R-S, Cao Q, Brenner CJ, Cao X *et al.* An integrated network of androgen receptor, polycomb, and TMPRSS2-ERG gene fusions in prostate cancer progression. *Cancer Cell* 2010; **17**: 443–454.
30 Zhang Y, Liu T, Meyer C, Eeckhoute J, Johnson D, Bernstein B *et al.* Model-based analysis of ChIP-Seq (MACS). *Genome Biol* 2008; **9**: R137.
31 Kryndushkin D, Wickner R, Shewmaker F. FUS/TLS forms cytoplasmic aggregates, inhibits cell growth and interacts with TDP-43 in a yeast model of amyotrophic lateral sclerosis. *Protein Cell* 2011; **2**: 223–236.
32 Minucci S, Maccarana M, Cioce M, De Luca P, Gelmetti V, Segalla S *et al.* Oligomerization of RAR and AML1 transcription factors as a novel mechanism of oncogenic activation. *Mol Cell* 2000; **5**: 811–820.
33 Boersema PJ, Raijmakers R, Lemeer S, Mohammed S, Heck AJR. Multiplex peptide stable isotope dimethyl labeling for quantitative proteomics. *Nat Protoc* 2009; **4**: 484–494.
34 Wilson NK, Foster SD, Wang X, Knezevic K, Schütte J, Kaimakis P *et al.* Combinatorial transcriptional control in blood stem/progenitor cells: genome-wide analysis of ten major transcriptional regulators. *Cell Stem Cell* 2010; **7**: 532–544.
35 Diffner E, Beck D, Gudgin E, Thoms JAI, Knezevic K, Pridans C *et al.* Activity of a heptad of transcription factors is associated with stem cell programs and clinical outcome in acute myeloid leukemia. *Blood* 2013; **121**: 2289–2300.
36 Beck D, Thoms JAI, Perera D, Schütte J, Unnikrishnan A, Knezevic K *et al.* Genome-wide analysis of transcriptional regulators in human HSPCs reveals a densely interconnected network of coding and noncoding genes. *Blood* 2013; **122**: e12–e22.
37 Martens JHA, Brinkman AB, Simmer F, Francoijs K-J, Nebbioso A, Ferrara F *et al.* PML-RARalpha/RXR alters the epigenetic landscape in acute promyelocytic leukemia. *Cancer Cell* 2010; **17**: 173–185.
38 Ebralidze AK, Guibal FC, Steidl U, Zhang P, Lee S, Bartholdy B *et al.* PU.1 expression is modulated by the balance of functional sense and antisense RNAs regulated by a shared cis-regulatory element. *Genes Dev* 2008; **22**: 2085–2092.

39 Pereira DS, Dorrell C, Ito CY, Gan OI, Murdoch B, Rao VN *et al.* Retroviral transduction of TLS-ERG initiates a leukemogenic program in normal human hematopoietic cells. *Proc Natl Acad Sci USA* 1998; **95**: 8239–8244.
40 Rapin N, Porse BT. Oncogenic fusion proteins expressed in immature hematopoietic cells fail to recapitulate the transcriptional changes observed in human AML. *Oncogenesis* 2014; **3**: e106.
41 Drach J, McQueen T, Engel H, Andreeff M, Robertson KA, Collins SJ *et al.* Retinoic acid-induced expression of CD38 antigen in myeloid cells is mediated through retinoic acid receptor-{alpha}. *Cancer Res* 1994; **54**: 1746–1752.
42 Drach J, Zhao S, Malavasi F, Mehta K. Rapid induction of CD38 antigen on myeloid leukemia cells by all trans-retinoic acid. *Biochem Biophys Res Commun* 1993; **195**: 545–550.
43 Dubois C, Schlageter M, de Gentile A, Guidez F, Balitrand N, Toubert M *et al.* Hematopoietic growth factor expression and ATRA sensitivity in acute promyelocytic blast cells. *Blood* 1994; **83**: 3264–3270.
44 Saeed S, Logie C, Stunnenberg HG, Martens JHA. Genome-wide functions of PML-RAR[alpha] in acute promyelocytic leukaemia. *Br J Cancer* 2011; **104**: 554–558.
45 Grignani F, De Matteis S, Nervi C, Tomassoni L, Gelmetti V, Cioce M *et al.* Fusion proteins of the retinoic acid receptor-[alpha] recruit histone deacetylase in promyelocytic leukaemia. *Nature* 1998; **391**: 815–818.
46 Lin RJ, Nagy L, Inoue S, Shao W, Miller WH, Evans RM. Role of the histone deacetylase complex in acute promyelocytic leukaemia. *Nature* 1998; **391**: 811–814.
47 De Bellis F, Carafa V, Conte M, Rotili D, Petraglia F, Matarese F *et al.* Context-selective death of acute myeloid leukemia cells triggered by the novel hybrid retinoid-HDAC inhibitor MC2392. *Cancer Res* 2014; **74**: 2328–2339.
48 Liu S, Klisovic RB, Vukosavljevic T, Yu J, Paschka P, Huynh L *et al.* Targeting AML1/ETO-histone deacetylase repressor complex: a novel mechanism for valproic acid-mediated gene expression and cellular differentiation in AML1/ETO-positive acute myeloid leukemia cells. *J Pharmacol Exp Ther* 2007; **321**: 953–960.
49 Saeed S, Logie C, Francoijs K-J, Frigè G, Romanenghi M, Nielsen FG *et al.* Chromatin accessibility, p300, and histone acetylation define PML-RARa and AML1-ETO binding sites in acute myeloid leukemia. *Blood* 2012; **120**: 3058–3068.
50 Sun Z, Diaz Z, Fang X, Hart MP, Chesi A, Shorter J *et al.* Molecular determinants and genetic modifiers of aggregation and toxicity for the ALS disease protein FUS/TLS. *PLoS Biol* 2011; **9**: e1000614.
51 Shikami M, Miwa H, Nishii K, Takahashi T, Shiku H, Tsutani H *et al.* Myeloid differentiation antigen and cytokine receptor expression on acute myelocytic leukaemia cells with t(16;21)(p11;q22): frequent expression of CD56 and interleukin-2 receptor α chain. *Br J Haematol* 1999; **105**: 711–719.
52 Denissov S, van Driel M, Voit R, Hekkelman M, Hulsen T, Hernandez N *et al.* Identification of novel functional TBP-binding sites and general factor repertoires. *EMBO J* 2007; **26**: 944–954.
53 Li H, Durbin R. Fast and accurate short read alignment with Burrows–Wheeler transform. *Bioinformatics* 2009; **25**: 1754–1760.
54 Li H, Handsaker B, Wysoker A, Fennell T, Ruan J, Homer N *et al.* The Sequence Alignment/Map format and SAMtools. *Bioinformatics* 2009; **25**: 2078–2079.

Supplementary Information accompanies this paper on the Oncogene website (http://www.nature.com/onc)